IOSR Journal of Applied Chemistry (IOSR-JAC)
e-ISSN: 2278-5736.Volume 19, Issue 9 Ser. I (September. 2026), PP 39-48
www.iosrjournals.org

Synthesis of a coordination polymer of manganese-potassium with *N*'-(1-(thiophen-2-yl)ethylidene)isonicotinohydrazide. Spectroscopic study, crystal structure determination and ATG study

Dame Gadiaga[a,b], Amar Diop[b], Adama Sy[a,b*], James Orton[c], Ibrahima Elhadji Thiam[b], Simon Coles[c], Ousmane Diouf[b] and Mohamed Gaye[b]

[a] *LSAO-MED, Gaston Berger University, Saint-Louis, Senegal*
[b]*Department of Chemistry, University Cheikh Anta Diop, Dakar, 10700, Senegal*
[c]*UK National Crystallography Service, School of Chemistry and Chemical Engineering, Faculty of, Engineering and Physical Sciences, University of Southampton, SO17, 1BJ, UK*

Abstract
*The functionalised hydrazide ligand, N'-(1-(thiophen-2-yl)ethylidene)isonicotinohydrazide (**HL**) has been synthesised and utilised to create a novel mixed-metal complex material [MnK(**HL**)$_4$(SCN)$_2$]Cl ½(MeOH) (**1**) at room temperature. This ligand acts in a η^1, η^1, η^1:μ_2-mode, bridging both Mn^{2+} and K^+ metal species into an extended 2D-network. The manganese ions form N_6 octahedra whereas the potassium ions are found in either distorted O_4N_4 square-antiprisms or highly irregular $O_4N_4S_4$ icosahedra. This variation of potassium environments results from disorder of the pendant thiophen-2-yl groups of the **HL** ligand found in a ratio close to 1:6. **1** crystallizes in the orthorhombic space group Ibam and is a Z' = 0.125 structure. This novel network material is hereby structurally characterized by elemental analysis, FTIR, UV-visible, conductance measurement, room temperature magnetic measurement and its single crystal X-ray diffraction (scXRD) structure is described. Thermogravimetric analysis (carried out at 25 - 700 °C) showed a three-stage decomposition pathway.*
***Keywords**: Crystal, manganese, potassium, octahedral, magnetism, TGA.*

Date of Submission: 08-09-2026 Date of Acceptance: 17-09-2026

I. Introduction

Hydrazine derivatives, particularly hydrazides, have attracted particular attention due to their biological activities, which can be enhanced after complexation with a metal ion [1,4]. Depending on the substituents used in the keto-precursors with which they are condensed, they can produce ligands of interest in coordination chemistry [5,9]. These ligands allow the synthesis of complexes with very varied structures. Indeed, discrete [10,11], dimeric [12,13], trimeric [14,15] or highly polymeric [16,17] structures can be produced during complexation with metal ions. Several complexes obtained from hydrazide derivatives have antifungal [18], antimicrobial [19], antituberculosis [20] or antitumor [21,22] properties. These complexes are also used in polymer coatings or pigments [23,26]. Some hydrazide derivatives are used in biomimetic chemistry due to their chelation mode, which is similar to the chelation mode with transition metal ions present in living systems [27,28]. Some coordination complexes act as enzyme inhibitors and are used for their pharmacological applications [29,32]. Several complexes with properties such as magnetism [33], luminescence [34], and catalysis [35] have been reported. Coordination complexes obtained from hydrazide derivatives exhibit supramolecular interactions because the main unit-C(O)NH-N=C-includes hydrogen bond donors and acceptors. Therefore, hydrogen bonding plays an important role in extending and stabilizing the structures of the resulting complexes [36,37]. In this work, we prepared the ligand *N*'-(1-(thiophen-2-yl)ethylidene)isonicotinohydrazide from isonicotinic hydrazide and 2-acetylthiophene. In addition to the classic donor atoms of the hydrazone unit (N,O), the ligand also contains a sulfur atom (S), which is a soft coordination site that can be complex with a metal ion. This ligand allowed the production of the complex [K(HL)$_4$Mn(SCN)$_2$]Cl ½(MeOH) (**1**) which is studied in this work.

* Corresponding author : adama.sy@ugb.edu.sn

II. Experimental

2.1. Materials and instruments

2-acetylthiophene-carboxaldehyde, isonicotinic hydrazide and manganese chloride heptahydrate were sourced commercially (Aldrich) and used without further purifications. Reagent grade solvents used in all cases, but where appropriate then further dried or purified by standard methods. Elemental analyses performed with a VxRio EL Instrument and the FTIR spectra obtained *via* a Perkin Elmer FTIR Spectrum Two (4000-400 cm^{-1}). The UV-Vis spectra collected upon Perkin-Elmer Lambda 365 UV/Visible spectrophotometer (1000–200 nm). ^{1}H and ^{13}C NMR spectra of the Schiff base, recorded in DMSO-d_6 with a BRUKER 500 MHz spectrometer at room temperature using TMS as an internal reference. Thermogravimetric analysis (TGA), by means of a METTLER TOLIDO connected to a computer, with a heating rate of 5 °C/min, between 25 and 700 °C. Molar conductance measurements achieved with a WTW LF-330 conductivity meter with a WTW conductivity cell, using 10^{-3} M solutions of the metal complexes in DMF, measured at 25 °C. Magnetic measurements performed at room temperature by using a Johnson Mattey scientific magnetic susceptibility balance (Calibrant: $Hg[Co(SCN)_4]$).

2.2. Synthesis of the ligand *N*'-(1-(thiophen-2-yl)ethylidene)isonicotinohydrazide (H*L*)

Isonicotinic hydrazide (3 g, 0.02287 mol) introduced into a 100 mL flask containing 30 mL of ethanol before adding 2-acetylthiophene-carboxaldehyde (2.887 g, 0.02287) pre-dissolved in 5 mL of ethanol and two drops of glacial acetic acid. The reaction mixture then refluxed for 3 hours. The clear solution thus obtained *via* hot filtration. Cooling yields a yellow precipitate, isolated by filtration and washed with ethanol. Analysis calculated for $[C_{12}H_{11}N_3OS]$ C, 58.75; H, 4.50; N, 17.11; S, 13.02. Found: C, 58.76; H, 4.52; N, 17.13; S, 13.07. Yield : 85 %. FTIR (ν, cm^{-1}): 3247 [ν(NH)] ; 1660 [ν(C=O) amide]; 1596 [ν(C=N)], 1548 - 1407 [(ν(C=N) + ν(C=C))], 1049 [ν(N-N)], 991, 856, 836, 748, 701 δ(C-H). RMN ^{1}H [DMSO : (δ, ppm)]: 7,10 - 7,78 (7H, H-Ar), 11,017 (s, 1H, OH-iminol); RMN ^{13}C [DMSO : (δ, ppm)]: 162,58 [(C-iminol)]; 144,57 (C=N); 122,27 - 154,08 (C_{Ar}) ; 15,56 (CH_3).

2.3. Synthesis of compound (1)

In a 100 mL flask containing 10 mL of methanol, H*L* ligand (0.2450 g, 1 mmol) was introduced. To this solution, 5 mL of a methanolic solution containing $MnCl_2{\cdot}7H_2O$ (0.2519 g, 1 mmol) and 5 mL of a methanolic solution containing KSCN (0.1939 g, 2 mmol) were added. The mixture was stirred at room temperature for two hours. The clear solution obtained was filtered and left to evaporate slowly. After two weeks, yellow crystals suitable for XRD analysis were collected. Yield 70%. Analysis calculated for $[C_{100}H_{88}K_2Mn_2N_{28}O_8S_{12}{\cdot}2(Cl){\cdot}CH_4O]$ C, 40.77; H, 3.75; N, 15.75; Cl, 2.81; S, 15.44. Found: C, 40.80; H, 3.73; N, 15.78; Cl, 2.85; S, 15.48. FTIR (ν, cm^{-1}): 3182, 3068, 2057, 1677, 1613, 1556, 1532, 1492, 1414, 1278, 1046, 837, 737, 723. Λ ($S{\cdot}cm^2{\cdot}mol^{-1}$) : 27 (fresh solution) and 30 (two weeks after). μ_{eff} = 4.03 μ_B.

2.4. Crystal Structure Determination

Crystals suitable for single-crystal X-ray diffraction, of the reported compound (**1**), were grown by slow evaporation of MeOH solution of the complex. Details of the crystal structure solution and refinement are given in Table 1. Diffraction data were collected using a Rigaku FRE+ equipped with Varimax confocal mirrors and UG2 Universal goniometer with graphite monochromatized MoKα radiation (λ = 0.71073 Å). All data were corrected for Lorentz and polarization effects. Complex scattering factors were taken from the program package SHELXTL [38]. The structures were solved by direct methods which revealed the position of all non-hydrogen atoms. All the structures were refined on F^2 by a full-matrix least-squares procedure using anisotropic displacement parameters for all non-hydrogen atoms [39]. H atoms (NH, OH, CH and CH_3 groups) were geometrically optimized and refined as riding model by AFIX instructions. Molecular graphics were generated using *ORTEP* [40].

Table 1. Crystal data and structure refinement for 1.

Chemical formula	$C_{101}H_{92}Cl_2K_2Mn_2N_{28}O_9S_{12}$
M_r	2485.72
Crystal system, space group	Orthorhombic, *Ibam*
Temperature (K)	100
a (Å)	13.0768 (1)
b (Å)	14.9489 (2)

c (Å)	28.3120 (3)
V (Å^3)	5534.54 (10)
Z	2
D_{calc} (gcm^{-3})	1.492
λ (MoK_α) (Å)	0.71075
μ (mm^{-1})	0.65
F(000)	2560
Crystal size (mm)	0.28 × 0.11 × 0.11
θ range (°)	2.069-36.316
Indices h, k, l	-21 ≤ h ≤ 21, -24 ≤ k ≤ 24, -47 ≤ l ≤ 47
T_{min}, T_{max}	0.882, 0.941
No. of measured reflections	99798,
Independent reflections	6813
Observed [$I > 2\sigma(I)$] reflections	6129
R_{int}	0.024
$R[F^2 > 2\sigma(F^2)]$	0.035
$wR(F^2)$	0.100
S	1.09
No. of reflections	6813
No. of parameters	243
No. of restraints	117
Final Indices [$I >= 2\ \sigma\ (I)$]	$R_1 = 0.0346$, $wR_2 = 0.0971$
Final R Indices (for all data)	$R_1 = 0.0393$, $wR_2 = 0.0997$
$\Delta\rho_{max}$, $\Delta\rho_{min}$ (e Å^{-3})	0.69, -0.63

III. Results and Discussions

3.1. General Study

The analytical data agree with the formulation of the ligand $C_{12}H_{11}N_3OS$, **H*L*** and complex material **1**. The IR spectrum of **H*L*** reveals the appearance of an intense band at 1660 cm^{-1} attributed to the ν(C=O) vibrations of the amide group. The band observed at 1596 cm^{-1} is attributed to the ν(C=N) vibrations of the imine group, and those appearing in the region 1548-1407 cm^{-1} are due to the ν(C=C) and ν(C=N) vibrations of the rings. The absorption bands located in the region 1384-1236 cm^{-1} are assigned to the ν(C-N) vibrations of the amide group, and the one observed at 1049 cm^{-1} is due to the ν(N-N) azomethine vibration. The presence of the C-N bond vibration indicates the existence of the ligand in its amide form in solid state. This is confirmed by the presence of the ν(NH) vibration at 3427 cm^{-1}. The deformation vibrations of the C-H_{Ar} bonds of the aromatic groups are observed in the region 991-600 cm^{-1}. Analysis of the ^{1}H NMR spectrum of the ligand reveals the presence of signals integrating the eleven protons of the ligand. The singlet observed at 2.39 ppm is assigned to the methyl protons of the methyl group of the ligand. The signals appearing in the 7.10-7.78 ppm region, integrating for seven protons, are attributed to the protons of the two aromatic groups. The signal appearing at 11.017 ppm in singlet form is due to the iminole proton [-N=C(OH)-] resulting from the iminolisation of the ligand in DMSO solution. The ^{13}C NMR spectrum of the ligand recorded in DMSO exhibits signals attributed to the carbon atoms of the ligand. The signal observed at 154.08 ppm is attributed to the C=N carbon atom of the azomethine function.

The signal observed at 162.58 ppm is attributed to the carbon atom of the iminol function [-N=C(OH)-]. This observation confirms the transformation of the amide group into an iminol group in DMSO solution. The signals of the carbon atoms of the two aromatic groups appear in the region 122.27 - 151 ppm.

After coordination, the infrared spectrum of **1**, shows a significant shift in the ν(C=O), $\nu(C=N)_{imine}$, and $\nu(C=N)_{pyridine}$ bands relative to those found for the free ligand. These bands appeared at 1660, 1596, and 1548 cm^{-1}, respectively, have shifted to 1667, 1613, and 1540 cm^{-1}. These facts indicate the involvement of the oxygen atom of the amide group and the nitrogen atoms of the imine group and pyridine in the coordination with the Mn(II) metal ions present in the solid-state structure. A narrow and intense band is noted in the spectrum of the complex at 2057 cm^{-1} and 737 cm^{-1} due to ν(C≡N) and ν(S-C) of the SCN anion coordinated to the metal ions *via* the nitrogen atom. Molar conductivity measurements of the complex taken from a freshly prepared millimolar solution of DMF and after two weeks of storage indicate that the complex is of neutral electrolyte according to Geary [41]. The very small variation of the values allows us to conclude that the complex is stable in solution in DMF. The UV-Vis absorption spectra of ***HL*** and the complex within **1** were measured in DMF solutions (10^{-5}·mol·L^{-1}) at room temperature. Two absorption bands are pointed at 292 nm and 324 nm in the UV-Vis spectrum of H*L*. These absorption are due to the π-π* transitions of the pyridine and the thiophene rings and the C=N bonds of intra-ligand [42], respectively. Upon complexation, the absorption peaks of the π-π* transition of the aromatic rings are bathochromically shifted in the spectrum of **1**, to 296 and 328 nm, respectively, likely resulting from the coordination of the ligand to the metal ion [43]. The new band at 338 nm in the spectrum of **1**, is attributed to π→π* of C=N azomethine [44] and the additional band at 382 nm belongs to the ligand to metal charge transfer (LMCT). The magnetic moment within compound (**1**) is 4.03 μ_B. This value agree with the presence of one uncoupled Mn^{2+} high-spin d^5 in octahedral environment [45].

3.2. Thermogravimetric analysis (TGA) study of compound (1)

Thermogravimetric analysis (TGA) performed on the compound up to 700°C shows that the complex is stable up to 156°C (Figure 1). The TGA spectrum of the compound shows three mass losses. Between 156°C and 211°C there is a mass loss of 3.44% corresponding to the departure of one methanol molecule and one thiocyanate anion (calculated mass loss, 3.62%). From 211°C to 389°C the mass loss of 32.66% corresponded to the loss of three ligand molecules and one thiocyanate (calculated mass loss, 31.90%). From 389°C to 700°C the mass loss was 13.75% corresponding to the loss of one ligand molecule and one thiocyanate unit (calculated mass loss, 14.53%).

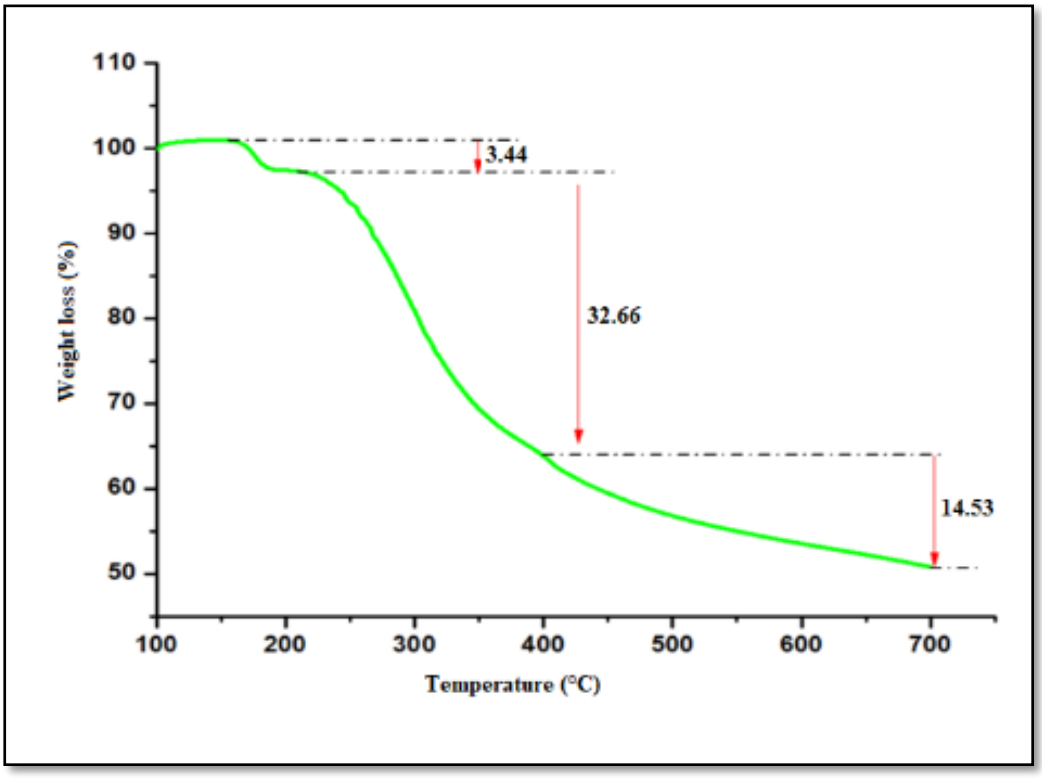

Figure 1 : *ATG(25 °C – 700° C) of compound (1).*

3.3. X-ray structure of compound (1)

The material formulated as $[K(HL)_4Mn(SCN)_2]Cl$ ½(MeOH) (**1**) crystallizes in the orthorhombic system with a space group *Ibam* to form a mixed-metal extended 2D-network. The crystal data collection and refinement are reported in Table 1. The asymmetric unit and numbering scheme is illustrated in Figure 2, with selected bonds lengths and angles are listed in Table 2. This is a $Z^{'}$=0.125, Z = 2 structure, the asymmetric unit contains a single ***HL*** ligand with the Mn^{2+}, K^{+}, and Cl^{-} ions sitting on special positions therefore crystallographically 25% occupied, the coordinated SCN^{-} ion is bisected by a mirror plane so 50% occupied and the solvent MeOH molecule straddles a glide plane, a screw axis and an inversion centre, and is necessarily 12.5% occupied. Within this structure, the ligand ***HL*** acts in η^1, η^1, η^1:μ_2-mode bridging one Mn^{2+} and the one K^{+} atoms. The sulfur atom and three of the four carbon atoms are disordered over two sites, with the occupancies major and minor occupancies freely refined to 0.8248(18) and 0.1752(18) respectively. The six-coordinated Mn centres are linked by four ligands through the nitrogen atom of pyridine ring (N1, $N1^{i}$, $N1^{ii}$, $N1^{iii}$) and two thiocyanate anions through their nitrogen atoms (N4, $N4^{i}$) to form a Jahn-Teller compressed octahedron as depicted in Figure 2.

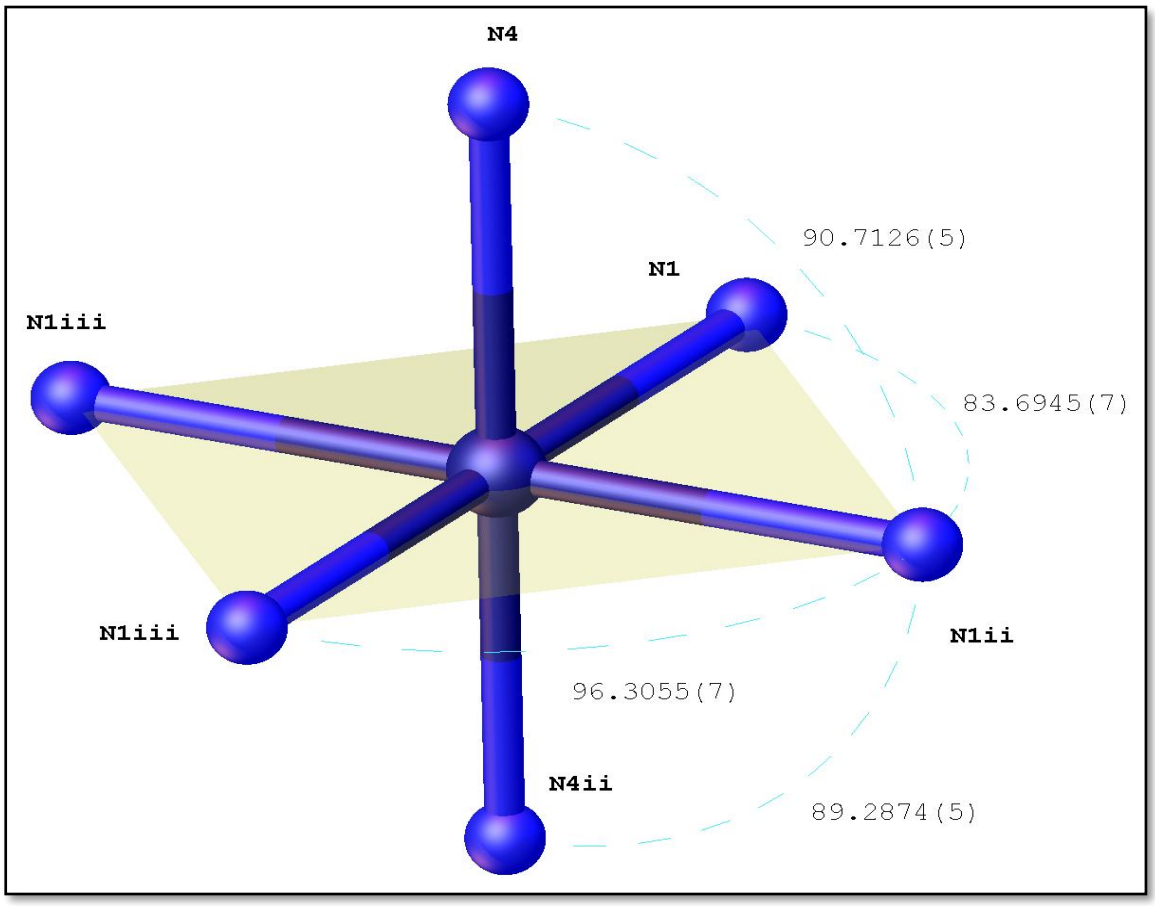

Figure 2. Illustration of the manganese coordination environment, with selected bond length and angles, where i = -x, 1-y, z; ii = -x, 1-y, 1-z; iii = x, y, 1-z

The basal Plane of the octahedron is comprised by the N4, $N4^{i}$, $N1^{ii}$ and $N1^{iii}$ atoms. The cissoid angles around the manganese atom which are in the range [89.29 (3)° - 90.71 (1)°], are close proximity to the ideal value of 90°. The diagonal basal angle values, $N1^{ii}$-Mn1-$N1^{iii}$ = 180.0° and N4-Mn1-$N4^{ii}$ = 180.0°, and the value of the angle subtended by the atoms in apical positions N1-Mn1-$N1^{i}$ = 180° are as the perfect value the ideal octahedral geometry. The manganese(II) ion lies nearly in the plane defined by N1, $N1^{i}$, $N1^{ii}$, $N1^{iii}$, the out-of-plane distance being 0.000 Å, with all Mn-$N_{pyridine}$ equal to 2.3093 (7) Å and Mn-$N_{thiocyanate}$ 2.1624 (2) Å. The whole anionic N-donor thiocyanates are quasi-linear with angle N-C-S in the range 179.53(13)°. These anionic N-donor thiocyanates bind not linearly to the manganese atom Mn-N-CS is 169.45 (11)°.

The potassium ion K1, is bound in two distinct environments, distorted square antiprism and an irregular dodecahedron resulting from the disordered thiophen-2-yl group. In the former, contacts to the carbonyl oxygen atom O1, the azomethine nitrogen atom N3 and by symmetry equivalent atoms $O1^{i}$, $O1^{ii}$, $O1^{iii}$ $N3^{i}$, $N3^{ii}$ and $N3^{iii}$. In the later arraigent there are three additional contacts to the major disordered position of S1a and its symmetry equivalent major disordered positions $S1A^{i}$ and $S1A^{ii}$. Bond lengths and angles of these contacts are summarised

in Table 2 and these two potassium environments are visualised in Figure 4. These distances are in the range reported for similar contacts [46-48] however such a mixed doner site involving potassium, oxygen, nitrogen and sulphur together is unusual.

Table 2. *Selected bond lengths (Å) and bond angles (°) for compound (1)*

Mn- $N_{pyridine}$	2.3093 (7)	N4 - Mn1 - $N4^{ii}$	180.0°
Mn - $N_{thiocyanate}$	2.1624 (2)	N1 - Mn1 - $N1^{iii}$	180°
N - C - S	179.53(13)°.	$N1^{ii}$ - Mn1 - $N1^{iii}$	180°
Mn - N - CS	169.45 (11)°	K2 - O1	2.7494 (7)
K2 - N3	3.4278 (8)	K2 - $O1^{i}$	2.7495 (7)
K2 - $N3^{i}$	3.4278 (8)	K2 - $O1^{ii}$	2.7494 (7)
K2 - $N3^{ii}$	3.4278 (8)	K2 - S1A	3.6392 (5)

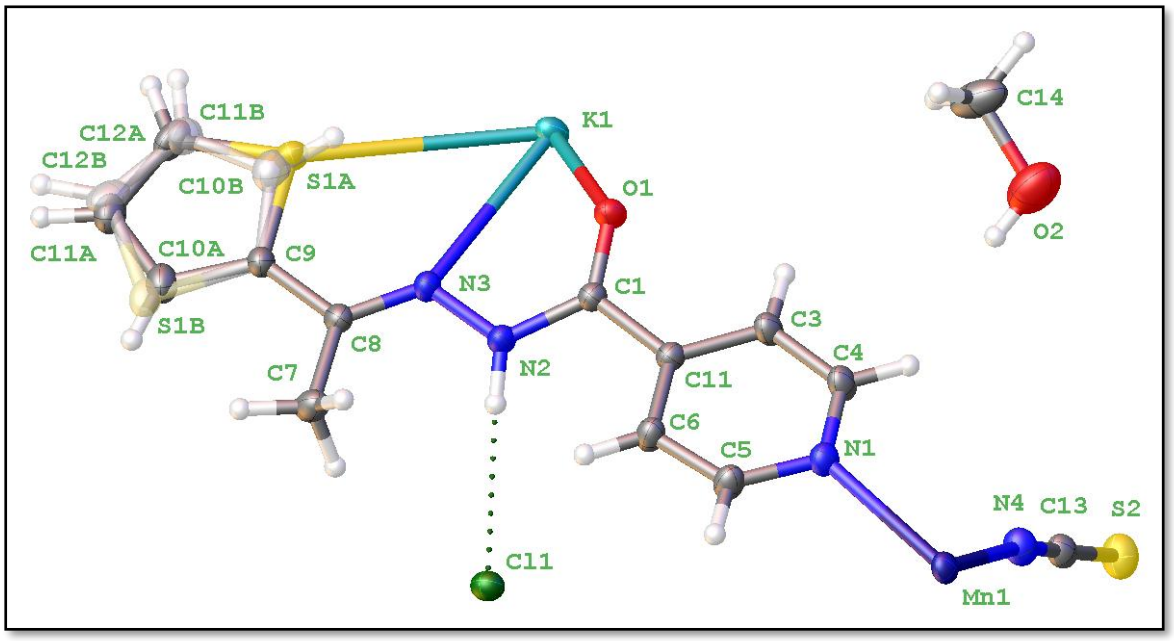

Figure 3. *numbering scheme and asymmetric unit structure of compound (1), thermal ellipsoids drawn at the 50% probability level, minor positions of the disordered thiophen-2-yl group drawn as ghosted (17.5%).*

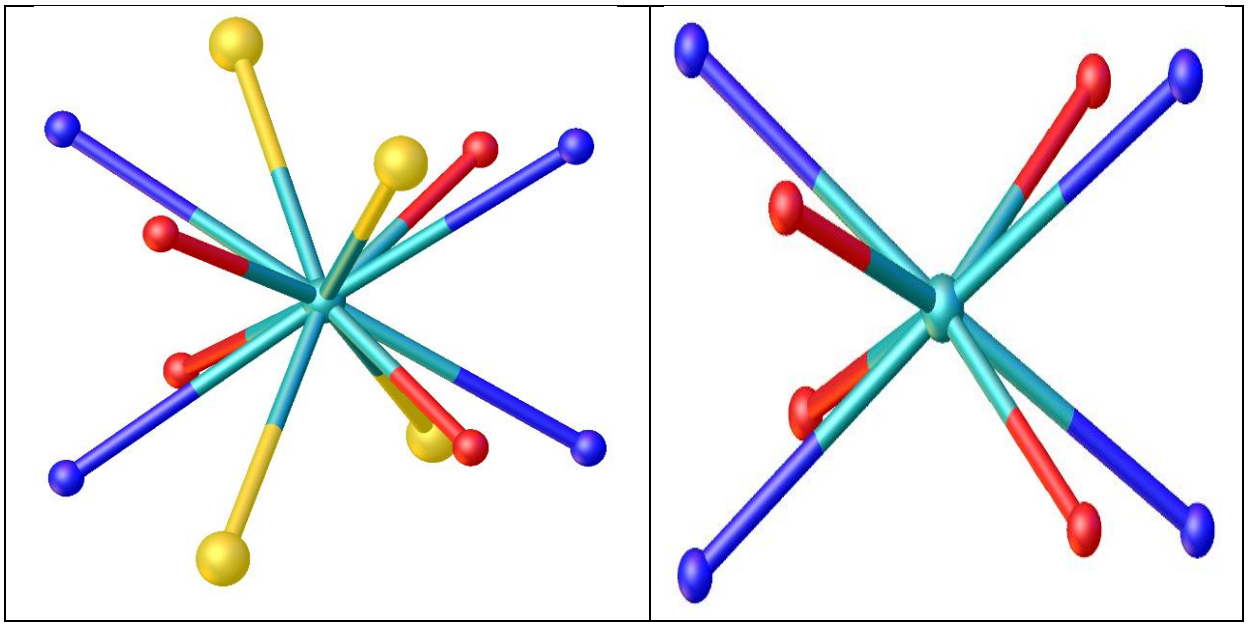

Figure 4. *Views of the two possible potassium ion environments [symmetry codes: to define].*

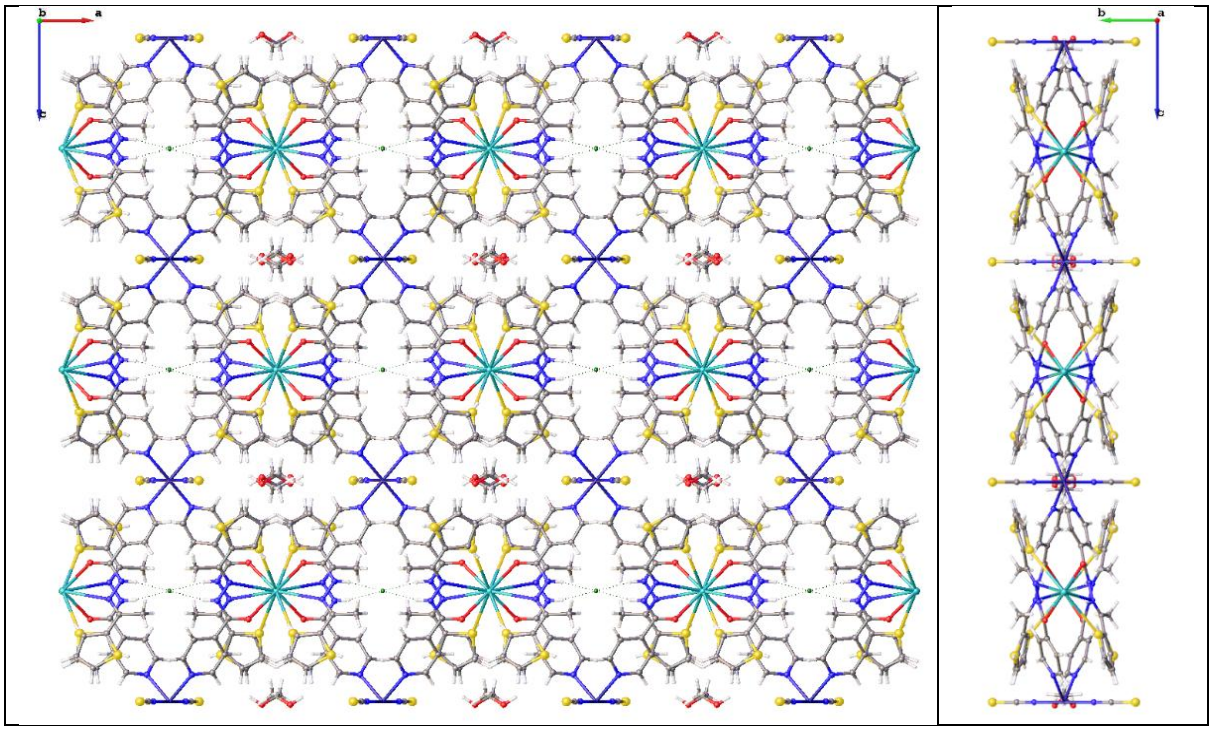

Figure 5. *Crystal packing of the title compound showing the arrangement parallel to the b axis (left) and parallel to a axis (right).*

IV. Conclusion

In the present work, we report the synthesis and characterization of a new complex of manganese prepared from the polydentate ligand *N*'-(1-(thiophen-2-yl)ethylidene)isonicotinohydrazide (H*L*). The ligand and the complex were characterized by NMR, FTIR, UV, conductance measurement and room temperature magnetic moment determination. The complex is a polymer. The FTIR spectral data showed that the ligand is coordinated with the metal center through the carbonyl oxygen atoms, the thiophen sulfur atoms and nitrogen atom of the pyridine ring. The electronic spectra show bands due to the ligand and the MLCT for complex **1**. Room temperature magnetic susceptibility measurement indicated that complex **1** is diamagnetic. Conductance measurement shows that complex **1** is non-electrolyte in nature. The structure of the complex within **1,** the ligand acts in η^1, η^1, η^1:μ_2-mode bridging one Mn(II) and one K(I) atoms, yielding an octahedral geometry of type N_6

for Mn(II) and a mixture of distorted square anti-prisms geometry of type O_4N_4 and irregular icosahedrons of type $O_4N_4S_4$.

Supporting information

CCDC-243648 contains the supplementary crystallographic data for this paper. These data can be obtained free of charge via https://www.ccdc.cam.ac.uk/structures/, or by emailingdata_request@ccdc.cam.ac.uk, or by contacting The Cambridge Crystallographic Data Centre, 12 Union Road, Cambridge CB2 1EZ, UK; fax: +44(0)1223-336033.

In Memoriam

Cheikh Halidou KANE 1963–2021. The death of Dr. KANE has deeply shocked us. Dr. KANE was a very talented chemist who was deeply involved in research and supervision of doctoral students. His contribution is greatly missed by our team. This article is dedicated to his memory.

References

[1]. Maurya RC, Patel P, Sutradhar D. Synthesis, Magnetic, Thermal, and Spectral Studies of Some Chelates of Cu(II), Ni(II), Zn(II), Co(II), Mn(II), Sm(III), and Th(IV) Involving Aroylhydrazones Derived from Isonicotinic Acid Hydrazide and 2-Furyl Methyl and 2-Thienyl Methyl Ketone. Synthesis and Reactivity in Inorganic and Metal-Organic Chemistry 2003;33(10):1857–1876. https://doi.org/10.1081/SIM-120026553

[2]. Vadankula GR, Nilkanth VV, Rizvi A, Yandrapally S, Agarwal A, Chirra H, Biswas R, Arifuddin M, Nema V, Mallika A, Mande SC, Banerjee S. Confronting Tuberculosis: A Synthetic Quinoline-Isonicotinic Acid Hydrazide Hybrid Compound as a Potent Lead Molecule Against Mycobacterium tuberculosis. ACS Infect Dis 2024;10(6):2288–2302. https://doi.org/10.1021/acsinfecdis.4c00277

[3]. Mir JM, Roy S, Vishwakarma PK, Maurya RC. cis-Dioxomolybdenum(VI) complex of N-o-hydroxyacetophenonene-isonicotinic acid hydrazide as nosocomial anti-infectious agent: experimental and theoretical study. Journal of the Chinese Advanced Materials Society 2018;6(3):282–300. https://doi.org/10.1080/22243682.2018.1466727

[4]. Tolan DA, Kashar TI, Yoshizawa K, El-Nahas AM. Synthesis, spectral characterization, density functional theory studies, and biological screening of some transition metal complexes of a novel hydrazide–hydrazone ligand of isonicotinic acid. Applied Organometallic Chemistry 2021;35(6):e6205. https://doi.org/https://doi.org/10.1002/aoc.6205

[5]. Judge V, Narasimhan B, Ahuja M, Sriram D, Perumal Y, Clercq ED, Pannecouque C, Balzarini J. Isonicotinic acid hydrazide derivatives: synthesis, antimicrobial activity, and QSAR studies. Medicinal Chemistry Research 2012;21(7):1451–1470. https://doi.org/10.1007/s00044-011-9662-9

[6]. Atta A, Fahmy S, Rizk O, Sriram D, Mahran MA. Structure-based design of some isonicotinic acid hydrazide analogues as potential antitubercular agents. Bioorganic Chemistry 2018;80:721–732. https://doi.org/10.1016/j.bioorg.2018.07.028

[7]. Lone MS, Mubarak MM, Nabi SA, Wani FR, Amin S, Nabi S, Kantroo HA, Samim M, Shafi S, Ahmad S, Ahmad Z, Rizvi SO. Isonicotinoyl-butanoic acid hydrazone derivatives as anti-tubercular agents: In-silico studies, synthesis, spectral characterization and biological evaluation. Medicinal Chemistry Research 2023;32(5):808–826. https://doi.org/10.1007/s00044-023-03039-5

[8]. Nassar H, Abou-El-Wafa MHM, Elkik H. Synthesis and characterization of some coordinated metal and charge transfer complexes of isonicotinic acid hydrazide ligand with 2-hydroxyacetophenonylidene. Spectrochimica Acta Part A: Molecular and Biomolecular Spectroscopy 2024;309:123759. https://doi.org/10.1016/j.saa.2023.123759

[9]. Amartey JK, Al-Jammaz I, Al-Otaibi B, Esguerra C. Novel synthesis of 2-[18F]-fluoroisonicotinic acid hydrazide and initial biological evaluation. Nuclear Medicine and Biology 2002;29(8):817–823. https://doi.org/10.1016/S0969-8051(02)00340-2

[10]. Cocu M, Bulhac I, Coropceanu E, Melnic E, Shova S, Ciobanica O, Gutium V, Bourosh P. Synthesis and structure of new mononuclear octahedral cobalt(III) dioximates derived from isonicotinic hydrazide. Journal of Molecular Structure 2014;1063:274–282. https://doi.org/10.1016/j.molstruc.2014.01.084

[11]. Abou-Melha KS. Transition metal complexes of isonicotinic acid (2-hydroxybenzylidene)hydrazide. Spectrochimica Acta Part A: Molecular and Biomolecular Spectroscopy 2008;70(1):162–170. https://doi.org/10.1016/j.saa.2007.07.023

[12]. Yin HD, Hong M, Wang QB, Xue SC, Wang DQ. Synthesis and structural characterization of diorganotin(IV) esters with pyruvic acid isonicotinyl hydrazone and pyruvic acid salicylhydrazone Schiff bases. Journal of Organometallic Chemistry 2005;690(6):1669–1676. https://doi.org/10.1016/j.jorganchem.2004.12.037

[13]. Kriza A, Ababei VL, Cioatera N, Rău I, Stănică N. Synthesis and structural studies of complexes of Cu, Co, Ni and Zn with isonicotinic acid hydrazide and isonicotinic acid (1-naphthylmethylene)hydrazide. Journal of the Serbian Chemical Society 2010;75(2):229–242. https://doi.org/10.2298/JSC1002229K

[14]. Mehla KA. Antimicrobial, spectral, magnetic and thermal studies of Cu(II), Ni(II), Co(II), UO_2(VI) and Fe(III) complexes of the Schiff base derived from oxalylhydrazide. Journal of Enzyme Inhibition and Medicinal Chemistry 2008;23(2):285–295. https://doi.org/10.1080/14756360701448073

[15]. Al-Shaalan NH. Synthesis, Characterization and Biological Activities of Cu(II), Co(II), Mn(II), Fe(II), and UO_2(VI) Complexes with a New Schiff Base Hydrazone: O-Hydroxyacetophenone-7-chloro-4-quinoline Hydrazone. Molecules 2011;16(10):8629–8645. https://doi.org/10.3390/molecules16108629

[16]. Singh VP, Tiwari K, and Mishra M. Synthesis, spectral and thermal studies of some polymeric mixed ligand uracil–hydrazide complexes with transition metal ions. Designed Monomers and Polymers 2013;16(5):456–464.

https://doi.org/10.1080/15685551.2012.747164
[17]. Slivkin AI, Lapenko VL, Bychuk AI, Suslina SN, Slivkin DA, Kornienko SV, Belenova AS. Polymeric Complexes of Isonicotinic Acid Hydrazide with Antituberculosis Effects. Bulletin of Experimental Biology and Medicine 2013;155(6):764–766. https://doi.org/10.1007/s10517-013-2247-5
[18]. Nfor EN, Husian A, Majoumo-Mbe F, Njah IN, Offiong OE, Bourne SA. Synthesis, crystal structure and antifungal activity of a Ni(II) complex of a new hydrazone derived from antihypertensive drug hydralazine hydrochloride. Polyhedron 2013;63:207–213. https://doi.org/10.1016/j.poly.2013.07.028
[19]. Bakale RP, Naik GN, Machakanur SS, Mangannavar CV, Muchchandi IS, Gudasi KB. Structural characterization and antimicrobial activities of transition metal complexes of a hydrazone ligand. Journal of Molecular Structure 2018;1154:92–99. https://doi.org/10.1016/j.molstruc.2017.10.035
[20]. Kumar B, Devi J, Dubey A, Tufail A, Taxak B. Investigation of antituberculosis, antimicrobial, anti-inflammatory efficacies of newly synthesized transition metal(II) complexes of hydrazone ligands: structural elucidation and theoretical studies. Scientific Reports 2023;13(1):15906. https://doi.org/10.1038/s41598-023-42180-4
[21]. Kocyigit-Kaymakcioglu B, Yazici SS, Tok F, Dikmen M, Engür S, Oruc-Emre EE, Iyidogan. Synthesis and Anticancer Activity of New Hydrazide-Hydrazones and Their Pd(II) Complexes. Letters in Drug Design & Discovery 2019;16(5):522–532. https://doi.org/10.2174/1570180815666180816124102
[22]. Ay B, Şahin O, Saygıdeğer Demir B, Saygideger Y, López-de-Luzuriaga JM, Mahmoudi G, Safin DA. Antitumor effects of novel nickel–hydrazone complexes in lung cancer cells. New J Chem 2020;44(21):9064–9072. https://doi.org/0.1039/D0NJ00921K
[23]. Aiken S, Gabbutt CD, Gillie LJ, Heywood JD, Jacquemin D, Rice CR, Heron BM. The Remarkable Hyperchromicity of Ketohydrazone Dyes and Pigment Lakes Derived from 4-Morpholino-2-naphthol. European Journal of Organic Chemistry 2013;2013(36):8097–8107. https://doi.org/10.1002/ejoc.201301218
[24]. Qian H-F, Geng J, Xu D, Huang W. Hydrazone to deprotonated azo/azo-enol transformation for isomeric pyrazolone based heterocyclic dyes via metal-ion complexation. Dyes and Pigments 2019;160:853–862. https://doi.org/10.1016/j.dyepig.2018.09.018
[25]. El-Wahab HA, El-Fattah MA, Ahmed AH, Elhenawy AA, Alian NA. Synthesis and characterization of some arylhydrazone ligand and its metal complexes and their potential application as flame retardant and antimicrobial additives in polyurethane for surface coating. Journal of Organometallic Chemistry 2015;791:99–106. https://doi.org/10.1016/j.jorganchem.2015.05.024
[26]. El-Wahab HA. The synthesis and characterization of the hydrazone ligand and its metal complexes and their performance in epoxy formulation surface coatings. Progress in Organic Coatings 2015;89:106–113. https://doi.org/10.1016/j.porgcoat.2015.08.001
[27]. Maurya RC, Rajput S. Neutral dioxovanadium(V) complexes of biomimetic hydrazones ONO donor ligands of bioinorganic and medicinal relevance: Synthesis via air oxidation of bis(acetylaceto-nato)oxovanadium(IV), characterization, biological activity and 3D molecular modeling. Journal of Molecular Structure 2007;833(1):133–144. https://doi.org/10.1016/j.molstruc.2006.09.022
[28]. Monfared HH, Kheirabadi S, Lalami NA, Mayer P. Dioxo- and oxovanadium(V) complexes of biomimetic hydrazone ONO and NNS donor ligands: Synthesis, crystal structure and catalytic reactivity. Polyhedron 2011;30(8):1375–1384. https://doi.org/10.1016/j.poly.2011.02.005
[29]. You Z, Yu H, Li Z, Zhai W, Jiang Y, Li A, Guo S, Li K, Lv C, Zhang C. Inhibition studies of Jack bean urease with hydrazones and their copper(II) complexes. Inorganica Chimica Acta 2018;480:120–126. https://doi.org/10.1016/j.ica.2018.05.020
[30]. Noma SAA, Erzengin M, Tunç T, Balcıoğlu S. Synthesis, characterization and biological assessment of a novel hydrazone as potential anticancer agent and enzyme inhibitor. Journal of Molecular Structure 2020;1205:127550. https://doi.org/10.1016/j.molstruc.2019.127550
[31]. Ayyannan G, Mohanraj M, Raja G, Bhuvanesh N, Nandhakumar R, Jayabalakrishnan C. New palladium(II) hydrazone complexes: Synthesis, structure and biological evaluation. Journal of Photochemistry and Photobiology B: Biology 2016;163:1–13. https://doi.org/10.1016/j.jphotobiol.2016.08.003
[32]. De Melo TRF, Chelucci RC, Pires MEL, Dutra LA, Barbieri KP, Bosquesi PL, Trossini GHG, Chung MC, Dos Santos JL. Pharmacological Evaluation and Preparation of Nonsteroidal Anti-Inflammatory Drugs Containing an N-Acyl Hydrazone Subunit. International Journal of Molecular Sciences 2014;15(4):5821–5837. https://doi.org/10.3390/ijms15045821
[33]. Biswas S, Das S, Rogez G, Chandrasekhar V. Hydrazone-Ligand-Based Homodinuclear Lanthanide Complexes: Synthesis, Structure, and Magnetism. European Journal of Inorganic Chemistry 2016;2016(20):3322–3329. https://doi.org/10.1002/ejic.201600335
[34]. Zheng C, Wang L, Liu J. Hydrothermal synthesis, structures, luminescence and magnetic properties of Zn(II) and Cu(II) complexes with new hydrazone ligand. Journal of Molecular Structure 2012;1018:78–83. https://doi.org/10.1016/j.molstruc.2011.11.008
[35]. Gayathri S, Viswanathamurthi P, Malecki JG, Bhavadharini A, Senthilkumar K. Copper(I) complexes with heteroaromatic hydrazone ligands: Synthesis, crystal structure and catalytic insights for tetrazole synthesis. Inorganica Chimica Acta 2025;575:122418. https://doi.org/10.1016/j.ica.2024.122418
[36]. Xia M, Cheng Y, Shang J, Leng X, Wei Z, Li Y. Biobased Self-healable Photoluminescent Polyacylhydrazones Imparted by Supramolecular Interactions. Macromolecules 2025;58(2):1077–1089. https://doi.org/10.1021/acs.macromol.4c02883
[37]. Kurbah SD, Umdor K. Nicotinohydrazide derived hydrazone ligated vanadium(V) complex: Supramolecular assembly and quantification of intermolecular interactions. Journal of Molecular Structure 2025;1321:139858. https://doi.org/10.1016/j.molstruc.2024.139858
[38]. Sheldrick GM. SHELXT – Integrated space-group and crystal-structure determination. Acta Crystallographica Section A 2015;71(1):3–8. https://doi.org/10.1107/S2053273314026370
[39]. Sheldrick GM. Crystal structure refinement with SHELXL. Acta Crystallographica Section C 2015;71(1):3–8. https://doi.org/10.1107/S2053229614024218
[40]. Farrugia LJ. WinGX and ORTEP for Windows: an update. Journal of Applied Crystallography 2012;45(4):849–854.

https://doi.org/10.1107/S0021889812029111
[41]. Geary WJ. The use of conductivity measurements in organic solvents for the characterisation of coordination compounds. Coordination Chemistry Reviews 1971;7(1):81–122. https://doi.org/10.1016/S0010-8545(00)80009-0
[42]. Li Y-J, Guo S-Z, Feng T, Xie K-F, Dong X-K. An investigation into three-dimensional octahedral multi-nuclear Ni(II)-based complexes supported by a more flexible salamo-type ligand. Journal of Molecular Structure 2021;1228:129796. https://doi.org/10.1016/j.molstruc.2020.129796
[43]. Wei Z-L, Wang L, Guo S-Z, Zhang Y, Dong W-K. A high-efficiency salamo-based copper(II) complex double-channel fluorescent probe. RSC Adv 2019;9(70):41298–41304; https://doi.org/10.1039/C9RA09017G.
[44]. Mansour AM. Selective coordination ability of sulfamethazine Schiff-base ligand towards copper(II): Molecular structures, spectral and SAR study. Spectrochimica Acta Part A: Molecular and Biomolecular Spectroscopy 2014;123:257–266. https://doi.org/10.1016/j.saa.2013.12.066
[45]. Tyagi M, Chandra S, Tyagi P. Mn(II) and Cu(II) complexes of a bidentate Schiff's base ligand: Spectral, thermal, molecular modelling and mycological studies. Spectrochimica Acta Part A: Molecular and Biomolecular Spectroscopy 2014;117:1–8. https://doi.org/10.1016/j.saa.2013.07.074
[46]. Mendoza-Báez R, Molina-Renteria A, Olguín J. Nitro group and K+-based secondary building units for the self-assembly of 3D coordination polymers built on dinuclear dianionic helicate connectors±. CrystEngComm, 2024;26:2346-2352. https://doi.org/10.1039/D4CE00255E
[47]. Azzam RA, Elgemeie GH, Osman RR, Jones PG. Crystal structure of potassium [4-amino-5-(benzo-[*d*]thiazol-2-yl)-6-(methylsulfanyl)pyrimidin-2-yl]-(phenylsulfonyl)azanide dimethylformamide monosolvate hemihydrate. Acta Crystallographica Section E. 2019;75:367–371. https://doi.org/10.1107/S2056989019002275
[48]. Kottalanka RK, Naktode K, Anga S, Panda TK. Synthesis and structure of potassium and barium complexes with diphenylphosphinothioicamido ligand containing Ba-S direct bonds. Phosphorus, Sulfur, and Silicon. 2014;189:1624–1632. https://doi.org/10.1080/10426507.2013.818998